Chin. J. Astron. Astrophys. Vol. 3 (2003), No. 6, 526–534
(*http://www.chjaa.org* or *http://chjaa.bao.ac.cn*)

Chinese Journal of Astronomy and Astrophysics

Extinction of Beamed Gamma-ray Burst Afterglows in a Dense Circumstellar Cloud*

Shun-Lin Liang, Zi-Gao Dai, Yong-Feng Huang and Tan Lu

Department of Astronomy, Nanjing University, Nanjing 210093; liangshunlin@sina.com; daizigao@public1.ptt.js.cn

Received 2003 April 28; accepted 2003 June 23

Abstract Broadband afterglow observations provide a probe of the density structure of the circumburst medium. In the spreading jet model, prompt and intense X-ray/UV radiation from the reverse shock may destroy and clear the dust in the circumburst cloud out to about 30 pc within the initial solid angle of the jet. As the jet expands significantly, optical radiation from the high-latitude part of the jet may suffer extinction by dust outside the initial solid angle, while radiation from the part within the initial solid angle can be observed without extinction. In previous studies, it is usually assumed that the extinction is complete. We calculate the extinction effect by taking the optical depth into account. Our numerical results show that a break appears in the light curve of optical afterglow but it extends over a factor of ~ 80 in time rather than a factor of ~ 10 in time for the case of strong dust extinction and a factor of ~ 60 in time for the case without dust extinction. These results may provide a way to judge how large the number density of the circumburst cloud is. Finally, we carry out a detailed modeling for the afterglow of GRB 000926. Our model can provide a good fit to the multi-color observations of this event.

Key words: gamma-rays: bursts — dust: extinction — stars: formation

1 INTRODUCTION

A current hypothesis suggests that long duration bursts arise from massive stars (e.g. via the collapsar scenario), while short bursts ($\lesssim 5$ s) may possibly be related to neutron star-neutron star(NS-NS) and neutron star-black hole(NS-BH) mergers (Katz & Canel 1996; Popham, Woosley & Fryer 1999; Lu et al. 2000; Cheng & Lu 2001; Qin et al. 2003). If GRBs emit up to 10^{53} erg in gamma-rays and X-rays in a few seconds, followed by an afterglow of X-ray (Costa et al. 1997), optical (van Paradijs et al. 1997) and radio (Frail et al. 2000), the progenitors of this kind of GRBs have been proved to be associated with massive stars and star-forming regions. The most direct evidence relating GRBs to massive stars is the observations of the afterglow of GRB 980425 (Galama et al. 1998; Kulkarni et al. 1998), GRB 980326

* Supported by the National Natural Science Foundation of China.

(Bloom et al. 1999) and GRB 970228 (Reichart 1999; Galama et al. 2000). Those bursts are considered to be associated with supernovae. Because GRBs are in the last phase of the evolution of massive stars, they do not live long enough to travel far from where they are born. From the effect of dust extinction, the question whether there is a large amount of dust in galaxies hosting GRBs can be examined.

If the progenitors of GRBs are indeed located in star-forming regions, then these GRBs are likely to be surrounded by gas and dust. Dai, Huang & Lu (2001) have suggested that prompt and intense X-ray/UV radiation from the reverse shock produced by the interaction of the jet with the cloud may destroy and clear the dust out to about 30 pc within the initial solid angle of the jet. A time-dependent photoionization which combines self-consistent metal evolution and dust destruction under an intense X-ray/UV radiation has been discussed (Perna & Lazzati 2002; Perna, Lazzati & Fiore 2002; Lazzati & Perna 2002). As the jet's sideways expansion becomes significant, most of the optical radiation from the high-latitude part of the jet may be absorbed by dust outside the initial solid angle of the jet, and only the radiation from the part within the initial solid angle can be observed without extinction. Dai et al. (2001) have assumed that the extinction is complete. Here we evaluate the extinction effect outside the initial solid angle by taking the optical depth into account and discuss a detailed modeling for the afterglow of GRB 000926. In Section 2, we describe the dynamical model. In Section 3, we analyze the extinction outside the initial passage. In Section 4, we discuss the effects of the parameters. We carry out a detailed modeling for the multi-color afterglow of GRB 000926 in Section 5, and give a brief discussion and a summary in the final Section.

2 DYNAMICS

To investigate the detailed evolution of the afterglow emission, we use the model described by Huang, Dai & Lu (1999) and the numerical code developed by Huang et al. (2000c). Let R be the radial coordinate in the burster frame, t the observer's time, γ the Lorentz factor, $\theta_{\rm j}$ the half-opening angle of the ejecta, $M_{\rm ej}$ the ejecta mass, and m the swept-up cloud mass. The dynamical evolution of the jet is described by (Huang et al. 2000a, c)

$$\frac{dR}{dt} = \beta c\gamma(\gamma + \sqrt{\gamma^2 - 1}), \tag{1}$$

$$\frac{d\theta_{\rm j}}{dt} = \frac{c_{\rm s}(\gamma + \sqrt{\gamma^2 - 1})}{R}, \tag{2}$$

$$\frac{dm}{dR} = 2\pi R^2(1 - \cos\theta_{\rm j})nm_{\rm p}, \tag{3}$$

$$\frac{d\gamma}{dm} = -\frac{\gamma^2 - 1}{M_{\rm ej} + \epsilon m + 2(1 - \epsilon)\gamma m}, \tag{4}$$

$$c_{\rm s}^2 = \frac{\hat{\gamma}(\hat{\gamma} - 1)(\gamma - 1)c^2}{1 + \hat{\gamma}(\gamma - 1)}, \tag{5}$$

where $\beta = \sqrt{1 - 1/\gamma^2}$ and $\hat{\gamma} \approx (4\gamma + 1)/(3\gamma)$ (Dai et al. 1999). If $\epsilon \to 0$, Eq. (4) turns out to express the conservation of energy: $(\gamma - 1)M_{\rm ej} + (\gamma^2 - 1)m =$ constant (Huang et al. 1999; van Paradijs et al. 2000). There are several advantages in this model. First, it is applicable to both radiative and adiabatic jets, and proper for both ultra-relativistic and non-relativistic phases. It even allows the radiative efficiency ϵ to change with time, so that it can trace the evolution of

a partially radiative jet (Dai, Huang & Lu 1999). Secondly, it considers the lateral expansion of the jet realistically. The evolution of the lateral speed (taken as the speed of sound) is given by a reasonable expression during both ultra-relativistic and non-relativistic phases (see Eq. (5)). Furthermore, it also takes into account many other effects, e.g., the cooling of electrons and the equal arrival time surfaces.

In order to calculate the total observed flux density, we should integrate over the equal arrive time surface (Waxman 1997; Sari 1997; Panaitescu & Mészáros 1998) determined by

$$t = \int \frac{1-\beta\mu}{\beta c} dR \equiv \text{ const} \tag{6}$$

within the jet boundaries (Moderski et al. 2000; Panaitescu & Mészáros 1999; Huang et al. 2000a, 2000c).

3 EXTINCTION OUTSIDE THE INITIAL PASSAGE

In this section we evaluate the extinction effect outside the initial solid angle by taking the optical depth into account. Cardelli et al. (1989) derived a meaningful average extinction law, $A(\lambda)/A(V)$, over the wavelength range $3.5\,\mu\text{m} \sim 0.125\,\mu\text{m}$, where $A(\lambda)$ is the absolute extinction and $A(V)$ the visual extinction. They also found that this law is applicable to both diffuse and dense regions of the interstellar medium in the above wavelength range. If GRB host galaxies are characterized by a dust-to-gas ratio similar to that of the Milky Way, then $A_{\rm V} = N_{\rm H}/(1.79 \times 10^{21}\ {\rm cm}^{-2})$ (Predehl & Schmitt 1995). The mean R_V-dependent extinction law takes the form $\langle A(\lambda)/A({\rm V})\rangle = a(x) + b(x)/R_{\rm V}$, where x is the reciprocal of wavelength, in units of $\mu{\rm m}^{-1}$, and $R_{\rm V}$ is about 3.1. For optical/NIR wavelengths regions ($1.1 \leq x \leq 3.3$), $a(x)$ and $b(x)$ are defined as,

$$\begin{aligned} a(x) = 1 &+ 0.17699y - 0.50447y^2 - 0.02427y^3 + 0.72085y^4 \\ &+ 0.01979y^5 - 0.77530y^6 + 0.32999y^7, \end{aligned} \tag{7}$$

$$\begin{aligned} b(x) = 1.41338y &+ 2.28305y^2 + 1.07233y^3 - 5.38434y^4 \\ &- 0.62251y^5 + 5.30260y^6 - 2.09002y^7, \end{aligned} \tag{8}$$

where $y = (x - 1.82)$.

Figure 1 illustrates the geometry of our model. The dust column density along the line of sight parallel to the jet axis is, $N_{\rm H} = n \cdot R \cdot \sin(\theta - \theta_0)/\sin\theta_0$, where n is the number density of dust, θ_0 the initial half opening angle and θ the angle of shocked material on the equal arrive time surface between θ_0 and $\theta_{\rm j}$. So the absolute extinction is

$$\begin{aligned} A(\lambda) &= A({\rm V}) \times [a(x) + b(x)/R_{\rm V}] \\ &= \frac{N_{\rm H}}{1.79 \times 10^{21}\ {\rm cm}^{-2}} \times [a(x) + b(x)/R_{\rm V}] \\ &= \frac{n \cdot R \cdot \sin(\theta - \theta_0)/\sin\theta_0}{1.79 \times 10^{21}\ {\rm cm}^{-2}} \times [a(x) + b(x)/R_{\rm V}], \qquad (\theta_0 < \theta < \theta_{\rm j}), \end{aligned} \tag{9}$$

and the observed flux is

$$F_{\rm obs}(\lambda) = F_{\rm int} \times 10^{-0.4A(\lambda)}, \tag{10}$$

where $F_{\rm int}$ is intrinsic flux.

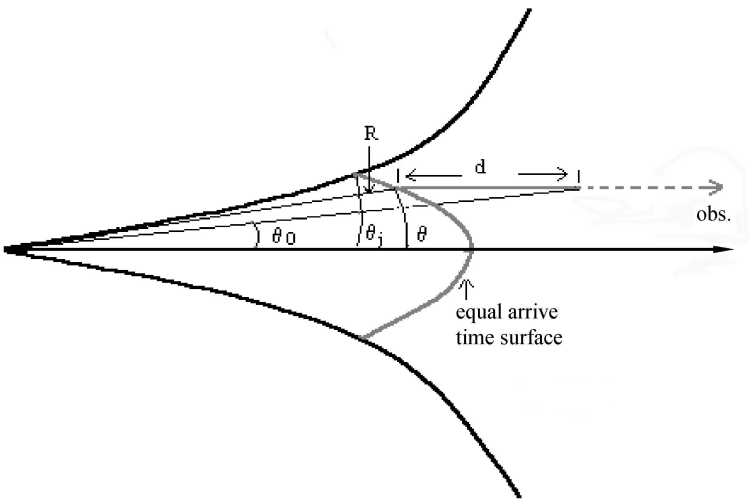

Fig. 1 Structure of a spreading jet expanding in a circumstellar cloud. Here θ_0 is the initial half opening angle, θ_j is the half opening angle, θ is the angle of shocked material on the equal arrival time surface between θ_0 and θ_j.

4 NUMERICAL RESULTS

Figure 2 presents light curves of R-band afterglow emission (p=2.5) for three cases with complete dust extinction (dashed line, Dai et al. 2001), partial dust extinction (solid line) and without dust extinction (dotted line, Huang et al. 2000a, b, c). This figure clearly shows that the light curve with partial dust extinction is located between the other two cases. When $t > 10^6$ s, the extinction effect becomes significant. Figure 3 exhibits $\alpha \equiv -d\ln F_R / d\ln t$ as a function of time for these three cases. In the case of complete dust extinction, α increases from ~ 1.3 at initial one day to ~ 3.2 at later times and the steepening is completed over a factor of ~ 10 in time. In the second case without dust extinction, α increases from ~ 1.3 at initial one day to ~ 2.5 and this change extends over a factor of ~ 60 in time. For the third case with partial dust extinction, α increases from ~ 1.3 at initial one day to ~ 2.8 at later times and this change extends over a factor of ~ 80 in time.

Figure 4 shows the effect of ISM number density n. According to analytical solutions under the ultra-relativistic assumption, the peak flux time t_p is not dependent on n. Figure 4 also shows that n affects the light curve steepening: with the increase of n, the extinction becomes larger and the time that the ejecta enters the Newtonian phase comes earlier, so that the light curve break becomes more and more striking. The effect of p on the light curves is shown in Figure 5, where p is the index characterizing the power-law energy distribution of electrons. With the increase of p, the break of the light curve becomes more significant and the break time becomes later. Figure 6 illustrates the effect of ε_e on the optical light curves, where ε_e is a parameter characterizing the efficiency of energy transport from protons to electrons. When ε_e is small, an obvious break does appear in the light curves. When ε_e is large, the break disappears. From Figure 6 we can see that with the increase of ε_e, the peak flux time becomes later but the light curves during the non-relativistic phase are almost characterized by the same

decay of $\alpha \simeq 2.8$. The effect of $\varepsilon_{\rm B}$ on the optical light curves is shown in Figure 7 and it is similar to that of $\varepsilon_{\rm e}$, where $\varepsilon_{\rm B}$ is the fraction of the thermal energy carried by magnetic field.

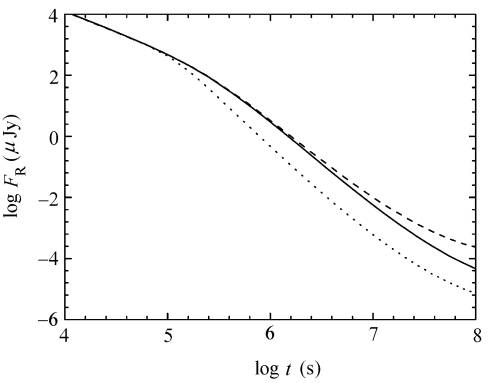

Fig. 2 R-band light curves of jetted GRB afterglows for no dust extinction (dashed line), partial extinction (solid line) and complete dust extinction (dotted line) cases. The model parameters are chosen as: $\epsilon = 10^{54}\,{\rm erg\ str^{-1}}$, $\gamma_0 = 300$, $\theta_0 = 0.15$, $p = 2.5$, $n = 10^3\ {\rm cm^{-3}}$, $\varepsilon_{\rm e} = 0.1$, $\varepsilon_{\rm B} = 10^{-6}$, and $D_{\rm L} = 10\,{\rm Gpc}$.

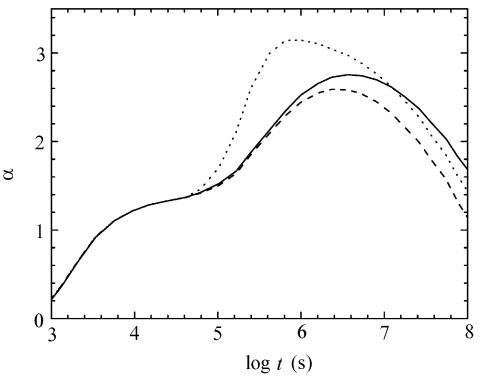

Fig. 3 R-band power-law index $\alpha \equiv -d\ln F_{\rm R}\,/d\ln t$ as a function of time. Parameters and line styles are the same as in Figure 2.

From the above, if the light curve has an obvious break during the relativistic phase, the parameter ε_e must be smaller than 0.5 but larger than 0.01, and ε_B must be smaller than 0.01. If these two conditions are satisfied, the light curves during the relativistic phase and non-relativistic phase are almost characterized by the same decay. So the parameters ε_e and ε_B have no direct effect on the extinction of the light curves. The parameter that produces the greatest effect on the extinction of the light curve is the dust density n.

5 AFTERGLOW OF GRB 000926

GRB 000926 was detected on 2000 September 26.9927 UT by the Inter-Planetary-Network (IPN) group of spacecraft Ulysses, Russian Gamma-Ray Burst Experiment (KONUS) and Near Earth Asteroid Rendezvous (NEAR) (Hurley et al. 2000). The burst had a 25–100 keV fluence of $\sim 2.2 \times 10^{-5}\ {\rm erg\,cm^{-2}}$. The total duration of the GRB is $\sim 25\,{\rm s}$, putting it in the class of long-duration bursts, to which all GRBs with detected afterglows so far belong (cf. Lamb 2000). The position was triangulated to a relatively small error box of approximately $35\,{\rm arcmin^2}$ and distributed to the GRB community 0.84 days after the burst (Hurley et al. 2000). The bright ($R \sim 19.5$) afterglow of GRB 000926 was identified by Gorosabel et al. (2000) and Dall et al. (2000) from observations taken less than a day after the burst. The redshift of the source was determined at $z = 2.0369 \pm 0.0007$ (Castro et al. 2000), yielding a luminosity distance of $D_{\rm L} = 16.9\,{\rm Gpc}$ ($H_0 = 65\,{\rm km\ s^{-1}\ Mpc^{-1}}$, $\Omega_{\rm m} = 0.3$, $\Omega_\lambda = 0.7$). Rol, Vreeswijk & Tanvir (2000) have fitted a late-time temporal slope of $\alpha = 3.2 \pm 0.4$. The existence of such achromatic breaks is usually taken to be a marked observational signature that the ejecta is not expanding isotropically, but rather highly collimated.

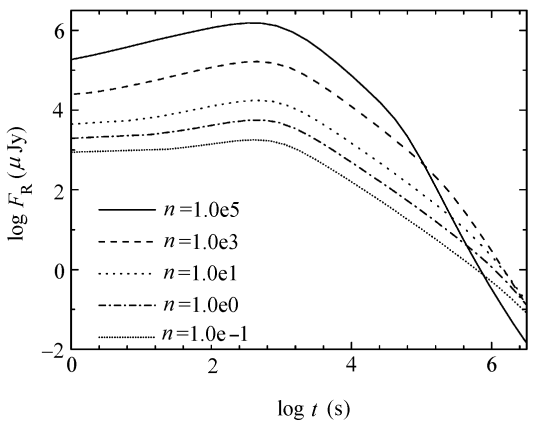

Fig. 4 Effects of dust density n on the light curves. The parameters are chosen as: $\epsilon = 8 \times 10^{53}$ erg str^{-1}, $\gamma_0 = 300$, $\theta_0 = 0.15$, $p = 2.5$, $\varepsilon_e = 0.1$, $\varepsilon_B = 4.8 \times 10^{-7}$, and $D_L = 16.9$ Gpc.

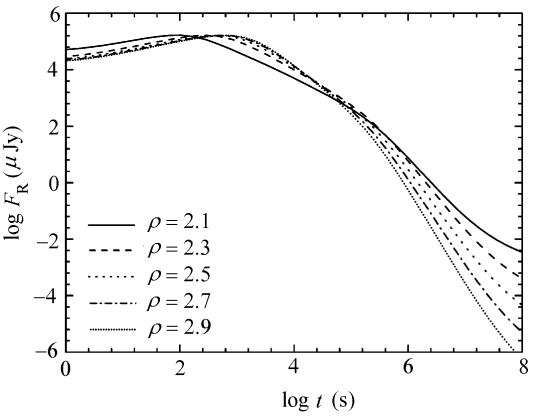

Fig. 5 Effects of p on the light curves. $n = 10^3$ cm^{-3} and other parameters are the same as in Figure 4.

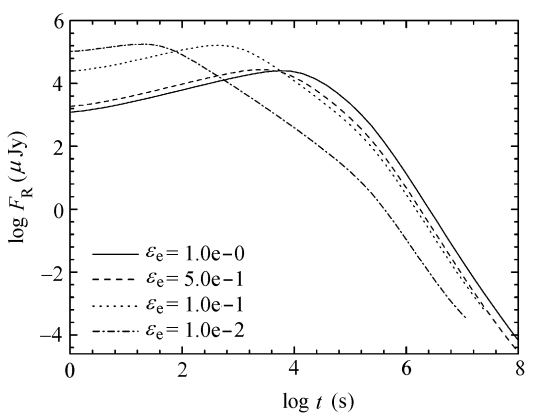

Fig. 6 Effects of ε_e on the light curves. $n = 10^3$ cm^{-3} and other parameters are the same as in Figure 4.

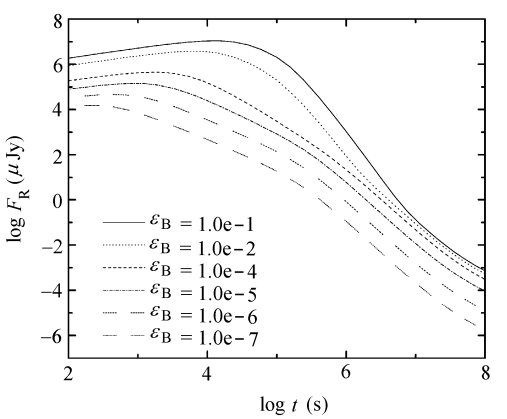

Fig. 7 Effects of ε_B on the light curves. $n = 10^3$ cm^{-3} and other parameters are the same as in Figure 4.

Multi-color light curves of the afterglows of GRB sources provide important information about the evolution of the relativistic blast wave expanding into the surrounding medium. If the broad-band light curves are observed at the time when the shock becomes non-relativistic, it can provide key physical parameters, including the total energy in the expanding ejecta, the density structure of the medium (Chevalier & Li 1999). Furthermore, the effects of dust as seen through extinction are easily observed in multi-color optical data. Dai et al. (2001) have fitted the observed R-band data of the afterglow by considering a simple jet model with dust extinction. Now we use our model to fit $BVRI$ optical monitoring of the afterglow of GRB 000926. Figure 8 shows the observed $BVRI$ optical data for GRB 000926 and the theoretically

calculated light curve based on the model described in Sections 2 and 3. It can be seen from this figure that our model provides a good fit to the multi-color afterglow data. More importantly, it is well described by a physical model where the spreading jet expands in a dense circumstellar cloud with dust density $\sim 10^3\,\mathrm{cm}^{-3}$. It can be the strong evidence linking the progenitors of GRBs with massive stars.

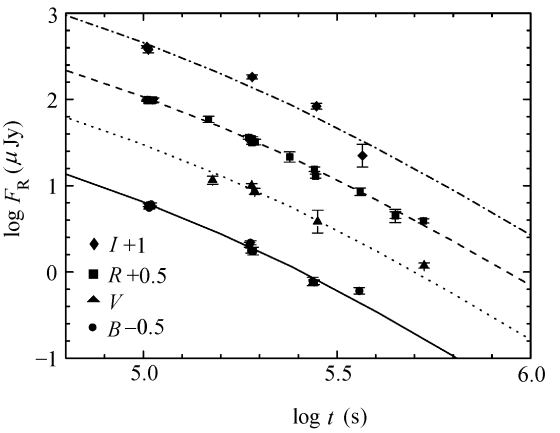

Fig. 8 A Comparison between the observed and theoretically calculated light curves for the $BVRI$ optical afterglow of GRB 000926. The observational data are taken from Price et al. (2001), and the model light curve is calculated for a spreading jet expanding in a circumstellar cloud when an observer is located on the jet axis. The model parameters are taken as: $\epsilon = 8 \times 10^{53}\,\mathrm{erg\ str}^{-1}$, $\gamma_0 = 300$, $\theta_0 = 0.15$, $p = 2.5$, $n = 10^3\ \mathrm{cm}^{-3}$, $\varepsilon_\mathrm{e} = 0.1$, $\varepsilon_\mathrm{B} = 4.8 \times 10^{-7}$, and $D_\mathrm{L} = 16.9\,\mathrm{Gpc}$.

6 DISCUSSION AND CONCLUSIONS

If a highly collimated fireball is expanding in a dense medium, two breaks in the light curve can be produced. The first is due to sideways expansion of a jet-like ejecta (e.g., Rhoads 1999; Wei & Lu 2000; Mao & Wang 2001; Gou et al. 2001; Zhang & Mészáros 2002; Huang et al. 2002). The second is attributed to a transition to non-relativistic phase due to the high density of the external medium, and is characterized by a flattening of the light curve. The presence of this feature indicates a large anisotropy in the original emission and the amount of energy release is reduced by a factor of ~ 100 relative to the isotropic value, which is consistent with the current stellar death models. On the evaluation of dust extinction outside the initial solid angle, our numerical results show that the break in the light curve of optical afterglow extends over a factor of ~ 80 in time. It implies that the additional emission from the outside of the initial solid angle can make the decline slower. In addition, we have given a good fit to the observed $BVRI$ data of the afterglow of GRB 000926.

How large is the dust density of the burst environment? On the assumption that GRBs trace cosmic star formation, Ramirez-Ruiz et al. (2002) have concluded that there may be clumps of dust which attenuate optical but not X-ray afterglow, if the column densities are between $10^{21} \sim 10^{23}\,\mathrm{cm}^{-2}$. To have noticeable effects on the X-ray spectrum, column densities of the order of $10^{23.5}\,\mathrm{cm}^{-2}$ or higher are required. If GRBs represent the final phase of evolution of massive stars which do not live long enough to leave their birth place, a large fraction are likely to be still enshrouded in their placental clouds of molecular gas and dust. Our result supports

the association of GRB with star forming region. For example, Ramirez-Ruiz et al. (2002) have shown that the interaction between the wind of a Wolf-Rayet star and a circumstellar medium of $n = 1\,\mathrm{cm}^{-3}$ leads to the formation of a quasi-uniform, hot shell, of density $\sim 10^3\,\mathrm{cm}^{-3}$, extending from $\gtrsim 10^{16}\,\mathrm{cm}$ up to $10^{18}\,\mathrm{cm}$. On the other hand, it is not as high as that required to produce the iron lines observed in some X-ray afterglows (e.g. Antonelli et al. 2001; Piro et al. 2000), which is possibly connected with much denser ($n \sim 10^{10}\,\mathrm{cm}^{-3}$) progenitor ejecta. An afterglow that lasts a few days requires a medium with a density $n \lesssim 10^7\,\mathrm{cm}^{-3}$.

Acknowledgements This research was supported by the Special Funds for Major State Basic Research Projects, the National Natural Science Foundation of China, the Foundation for Authors of National Excellent Doctoral Dissertation of P. R. China (Project No: 200125), and the National 973 Projects (NKBRSFG 19990754).

References

Antonelli L. A. et al. 2000, ApJ, 545, L39
Bloom J. S. et al. 1999, Nature, 401, 453
Cardelli J. S., Cayton G. C., Mathis J. S., 1989, ApJ, 345, 245
Castro S. M. et al. 2000, GCN, 851
Cheng K. S., Lu T., 2001, Chin. J. Astron. Astrophys, 1, 1
Chevalier R. A., Li Z. Y., 1999, ApJ, 520, L29
Costa E. et al., 1997, Nature, 387, 783
Dai Z. G., Huang Y. F., Lu T., 1999, ApJ, 520, 634
Dai Z. G., Huang Y. F., Lu T. 2001, MNRAS, 324, L11
Dall T. et al., 2000, GCN, 804
Frail D. A., waxman E., Kulkarni S. R., 2000, ApJ, 537, 191
Galama T. J. et al., 1998, Nature, 398, 394
Galama T. J. et al., 2000, ApJ, 536, 185
Gorosabel J., Castro Ceron J. M., Castro-Tirado A. J., Greiner J., 2000, GCN, 803
Gou L. J., Dai Z. G., Huang Y. F., Lu T., 2001, Chin. Astron. Astrophys, 25, 29
Huang Y. F., Dai Z. G., Lu T., 1998, A&A, 336, L69
Huang Y. F., Dai Z. G., Lu T., 1999, MNRAS, 309, 513
Huang Y. F., Dai Z. G., Lu T., 2000a, MNRAS, 316, 943
Huang Y. F., Dai Z. G., Lu T., 2000b, A&A, 355, L43
Huang Y. F., Gou L. J., Dai Z. G., Lu T., 2000c, ApJ, 543, 90
Huang Y. F., Tan C. Y., Dai Z. G., Lu T., 2002, Chin. Astron. Astrophys, 43, 169
Hurley K., Mazets E., Golenetskii S., 2000, GCN, 801
Hurley K., Mazets E., Golenetskii S., 2000, GCN, 802
Hurley K., Mazets E. et al., 2000, ApJ, 534, L23
Katz J. I., Canel L. M., 1996, ApJ, 471, 915
Kommers J. M. et al., 2000, ApJ, 533, 696
Kulkarni S. R. et al., 1998, Nature, 395, 663
Lamb D. Q., 2000, Phys. Rep., 333, 505
Lazzati D., Perna R., 2003, MNRAS, 340, 694
Lu Y., Zheng G. S., Zhao G., 2000, Chin. Phys. Lett., 17, 73
Mao J. R., Wang J. C., 2001, Chin. J. Astron. Astrophys, 1, 433
Moderski R., Sikora M., Bulik T., 2000, ApJ, 529, 151
Panaitescu A., Mészáros P., 1998, ApJ, 493, L31

Panaitescu A., Mészáros P., 1999, ApJ, 526, 707
Perna R., Lazzati D., 2002, ApJ, 580, 261
Perna R., Lazzati D., Fiore F., 2003, ApJ, 585, 775
Piro L. et al., 2000, Science, 290, 955
Popham R., Woosley S. E., Fryer C., 1999, ApJ, 518, 356
Predehl P., Schmitt J. H. M. M., 1995, A&A, 293, 889
Price P. A. et al., 2001, ApJ, 549, L7
Qin Y. P. et al., 2003, Chin. J. Astron. Astrophys, 3, 38
Ramirez-Ruiz E., Trentham N., Blain A. W., 2002, MNRAS, 329, 465
Reichart D. E., 1999, ApJ, 521, L111
Rhoads J. E., 1999, ApJ, 525, 737
Rol E., Vreeswijk P. M., Tanvir N., 2000, GCN Circ., 850
Sari R., 1997, ApJ, 494, L49
van Paradijs J. et al., 1997, Nature, 386, 686
van Paradijs J., Kouveliotou C., Wijers R. A. M. J., 2000, ARA&A, 38, 379
Waxman E., 1997, ApJ, 491, L19
Wei D. M., Lu T., 2000, ApJ, 541, 203
Zhang B., Mészáros P., 2002, ApJ, 571, 876